Design of a static synchronous compensator for the north-south high-speed railway system

An Thi Hoai Thu Anh[1], Tran Hung Cuong[2]
[1]Department of Electrical Engineering, Faculty of Electrical and Electronics Engineering, University of Transport and Communications, Hanoi, Vietnam
[2]Department of Electrical Engineering and Electronics, Faculty of Electrical and Electronic Engineering, Thuyloi University, Hanoi, Vietnam

Article Info	ABSTRACT
	The modern high-speed rail system plays a crucial role in driving the nation's economic development. The problem of voltage imbalance caused by intermittent load movements is a significant challenge for energy management and distribution. When electric trains are connected to the three-phase grid, power quality degradation occurs, resulting in distortion and imbalance of the three-phase grid current and voltage, which in turn increases operating costs. This paper has proposed a linear control method using a PI controller for a static synchronous compensator (STATCOM) to directly control the amount of reactive power loss for electric trains. This solution will also bring good and stable voltage quality to electric trains so that electric trains can operate for a long time. The STATCOM device in this paper is a three-phase voltage source converter with a simple structure and can be easily controlled. This is considered a simple and effective solution to balance voltage, improve power factor, and enhance harmonic quality for railway trains, thereby achieving an optimal operating solution. This discussion can be simulated using MATLAB/Simulink software to determine the operation and control steps for STATCOM, thereby improving the quality of the power system. The simulation results of current, voltage, and reactive power response are presented. The simulation results have demonstrated that the proposed algorithm successfully achieves the set goals of ensuring voltage stability and providing the necessary amount of reactive power for the train, thereby improving the quality of the power grid for the North-South high-speed train in Vietnam.

Corresponding Author:

Tran Hung Cuong
Department of Electrical Engineering and Electronics, Faculty of Electrical and Electronic Engineering
Thuyloi University
Hanoi, Vietnam
Email: cuongth@tlu.edu.vn

1. INTRODUCTION

The North-South high-speed railway system is a key project of Vietnam and is the first choice of countries worldwide. This system makes contributions to developing the economy of passenger transport and improving traffic [1]. However, the system requires a stable [2], [3]. When using electricity from the three-phase grid, current railway power systems often exhibit low reliability and poor flexibility, frequently encountering issues such as power imbalance, voltage fluctuations, and the presence of harmonics when connected to the grid [4]. These factors not only reduce the efficiency of train operation but also negatively affect the quality of electricity in the entire power system [5]-[7]. For electric trains to operate with power

from the grid, transformers are indispensable components to generate the voltage value required for train operation. However, in train systems with many continuously changing operating modes, transformers cannot respond quickly to the requirements of instantaneous power adjustment, voltage stabilization, and harmonic suppression [8]. Therefore, for high-speed railway trains to operate efficiently, more advanced solutions are necessary to ensure the system's performance and reliability. One of the most effective solutions today is to use a static synchronous compensator (STATCOM) to stabilize voltage and balance reactive power [9]-[11]. In the context of Vietnam's North-South high-speed railway system, which has large power consumption and stable operation requirements, the application of STATCOM not only helps to overcome current problems but also ensures that the system can meet future needs. STATCOM is a reactive compensation device based on power electronics conversion technology [9]. This device will be connected to the transformer supplying the train at the PCC point. Its task is to provide the reactive power required quickly by the railway train [12].

The advantage of the STATCOM device is that it responds quickly to requests for reactive power mobilization to stabilize the voltage and ensure optimal operating conditions for the train [13], [14]. STATCOM is capable of balancing the current, regulating the voltage, increasing the power factor, and minimizing harmonic currents in the system. Furthermore, the flexible, compact design and multi-objective capability of STATCOM have made it an ideal solution for improving the quality of railway trains [15], [16]. Previously, STATCOM has been widely studied and applied in various fields of power systems. The voltage stability control strategy based on reactive power compensation from STATCOM for wind farms to overcome voltage imbalance was introduced in [17]. Researcher in [15] showed that STATCOM can well control the value of reactive power supplied to the grid from wind farms. To improve the operating efficiency of industrial motors in the case of reactive power shortage, the reactive power compensation process at the load node was introduced in [18].

Currently, solutions to compensate for reactive power for high-speed railways are an urgent issue to improve the operational efficiency of electric trains and save operating costs. Reactive power compensation for electric trains requires acting quickly in all high-speed railway train operating modes. To do that, this paper will design a reactive power compensation system based on a three-phase voltage source converter connected at the point of common coupling (PCC) point supplying power to the train. Many control algorithms can act on the three-phase voltage source converter to compensate for reactive power and stabilize the terminal voltage for the train. Specifically: sliding mode control (SMC), model predictive control (MPC), and linear control (PI). SMC and MPC systems often provide better response and better control quality. Still, the disadvantage of these methods is that they are very complicated to implement on large systems such as high-speed railway systems, requiring measurement of many input parameters, making the system complex and expensive, and putting pressure on the microcontroller system. Meanwhile, the PI controller has a simple design and operation, few control inputs, but still provides good quality to meet the control goals, which is very suitable for operating high-speed railway systems with large distances of up to thousands of kilometers.

In this paper, the reactive power compensation control process is designed with two control loops using a PI linear controller, in which the outer loop adjusts the direct current (DC) and alternating current (AC) voltages of the three-phase bridge converter to bring the operating voltages to their reference values during operation. The inner control loop will control the current and reactive power to compensate for the power shortage required by the train. The selection of the PI controller in this system is to create a simple implementation process while still ensuring control requirements. At the same time, PI is a linear controller applied in many control systems of frequency converters [19]. PI can respond quickly, eliminate errors well, operate reliably, and stably [20]. Especially when programming microcontrollers, PI takes up few resources and has a small computational volume [21], [22]. This will help the system respond quickly; electronic devices can operate stably for a long time.

In this paper, the parameters of the PI controller are calculated and designed so that the controller can operate within the allowable ranges when the grid power system fluctuates due to objective reasons, or when the load of the train changes under different operating conditions. This feature has shown the advantage of the proposed method when applied to the load of the train, which has not been studied before in Vietnam or in developing countries like Vietnam. The system demonstration process was simulated and programmed using MATLAB/Simulink software. The results demonstrated the STATCOM system's voltage stability when supplying power to trains operating in different modes, with a deviation of no more than 5% compared to the rated value. The results also showed that the reactive power was controlled closely to the reference value required by the train in different operating modes with a minimal response time. The above results allowed the system to stabilize the reactive power balance and maintain voltage stability at the PCC point. This is the basis for developing energy operation systems for high-speed railway trains in Vietnam and worldwide.

2. OPERATING PRINCIPLE OF STATCOM FOR HIGH-SPEED RAILWAY TRAINS

The STATCOM device is connected in parallel with the train power supply system at the PCC point, as shown in Figure 1. This is to compensate for the reactive power of the train in case the train loses

voltage stability at the PCC point or there is a shortage of reactive power that the grid cannot provide. As is known, high-speed trains operate well thanks to a sufficient power supply with good power quality. Even small voltage fluctuations can affect the movement of high-speed trains. Two factors cause voltage fluctuations for high-speed trains: reactive power shortage and train speed (load changes) [23].

In this model, the reactive power mobilized for the train must be balanced with the reactive power required by the train, which means that to ensure the train's good operation. The grid power system, combined with STATCOM, must provide enough power for the train to ensure this requirement. The main part of STATCOM is a three-phase voltage converter, as demonstrated in Figure 2. Where Figure 2(a) is the schematic diagram of STATCOM connected to a three-phase grid, Figure 2(b) is the alternative diagram of STATCOM connected to a three-phase grid, and Figure 2(c) is the simplified diagram of Figure 2(b). The power transformer is represented by the inductor X.
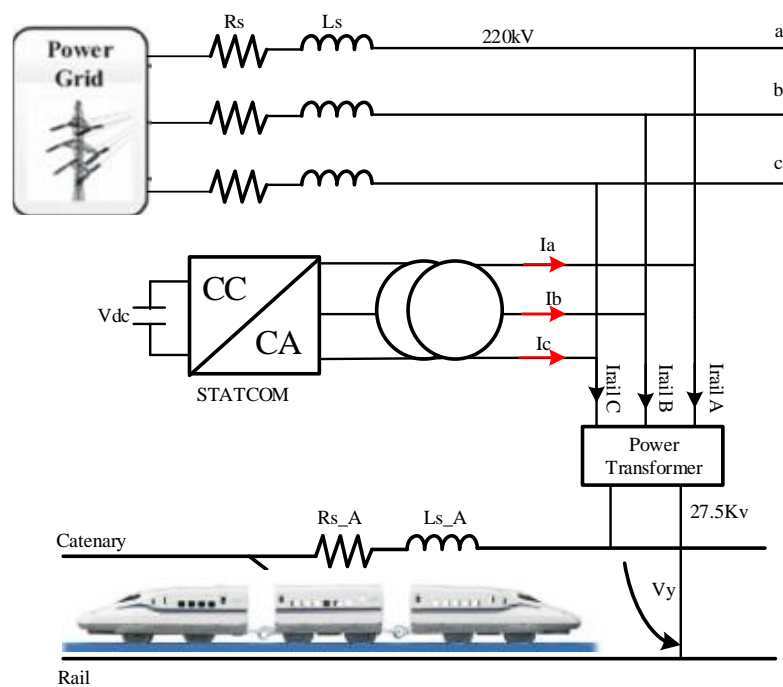
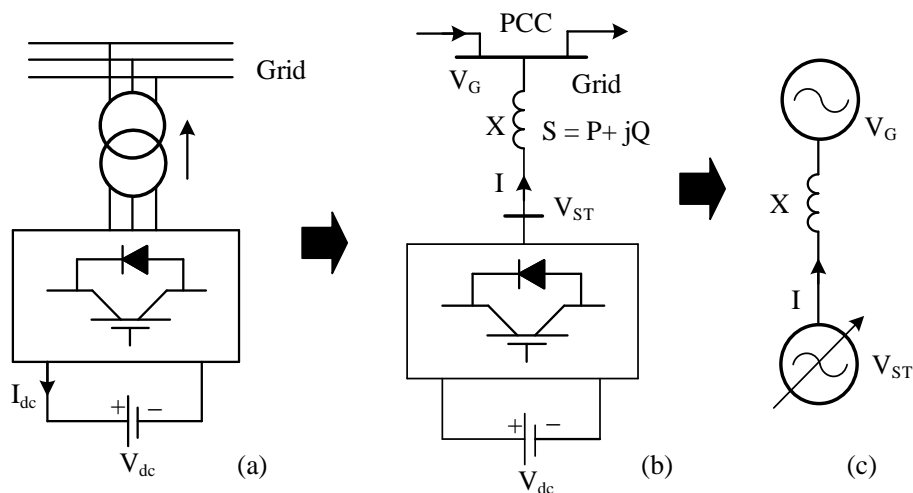Figure 1. General diagram of the STATCOM compensation system for trains

Figure 2. Equivalent circuit diagram of STATCOM

The (1) and (2) show the values of active power P and reactive power Q supplied to the train.

$$P = V_G I cos\varphi = \frac{V_{ST}V_G}{X}sin\delta \tag{1}$$

$$Q = V_G I sin\varphi = \frac{V_{ST}V_G}{X}cos\delta - \frac{V_G^2}{X} \tag{2}$$

In which: V_G is the voltage at the PCC point, V_{ST} is the voltage of STATCOM, δ is the phase angle between V_G and V_{ST}, φ is the phase angle between I_G and V_G. When the train operates stably and the power consumed by the train is fixed, the relationship between reactive power and other components in the system is written in (3).

$$Q = \sqrt{\left(\frac{V_{ST}V_G}{X}\right)^2 - P^2} - \frac{V_G^2}{X} \tag{3}$$

From (3), we see that the relationship between voltage and reactive power required by the train is written in the form of (4).

$$Q = \frac{V_G^2}{X} \tag{4}$$

In reality, high-speed trains operate in many modes, such as accelerating, decelerating, holding, and even stopping to pick up and drop off passengers. Therefore, the power consumption capacity of the train is different. This leads to different reactive power consumption modes. If the power supply's reactive power does not meet the operating modes of the train, the reactive power will decrease, causing the V_G voltage at the PCC point also to reduce. At this time, reactive power will be mobilized from the STATCOM device to ensure the balance of reactive power for the train. This is to avoid power shortage incidents that affect the operation of the train. From here, the voltage supplied to the train will have to increase to the rated value.

In permanent operation, the V_{ST} voltage generated by D-STATCOM matches the V_G voltage of the grid. In STATCOM mode with only reactive power compensation, $P_{ST} = 0$. Considering (1), the angle $\delta = 0$ achieves this. The (2) shows the amount of reactive power generated from STATCOM to supply the train (5).

$$Q_{ST} = \frac{V_{ST}V_G}{X} - \frac{V_G^2}{X} = \frac{V_G(V_{ST}-V_G)}{X} \tag{5}$$

The (5) shows that the reactive power of the train can be controlled by controlling the voltage supplied to it. When the reactive power supplied to the train decreases, the voltage will be controlled to increase to achieve the required reactive power value. The current absorbed by the STATCOM in Figure 2 is shown as (6) [24].

$$I = \frac{\dot{V}_G - \dot{V}_{ST}}{jX} \tag{6}$$

Here, V_G and V_{ST} always operate in phase and at the same frequency without being affected by the power losses caused during operation. Then, the reactive power Q_{ST} absorbed or emitted by the STATCOM device can be expressed as (7).

$$Q_{ST} = Im\left(\dot{V}_G \frac{(\dot{V}_G - \dot{V}_{ST})}{-jX}\right) = \frac{V_G(V_G - V_{ST})}{X} \tag{7}$$

From (7), we see that when the phases are the same, the V_{ST} can be controlled through the current and phase angle of the STATCOM. Accordingly, if the voltage at the PCC is greater than the output voltage of the STATCOM, the phase of the current from the system to the STATCOM will be 90º behind the voltage at the PCC. The STATCOM will operate in inductive mode and absorb the excess reactive power supplied to the high-speed train [25]. If the voltage at the PCC is less than the output voltage of the STATCOM, the phase of the current from the system to the STATCOM will be 90º ahead of the voltage at the PCC. The STATCOM will operate in capacitive mode and supply the necessary amount of reactive power to the train, as shown in Figure 3. Figure 3(a) shows STATCOM absorbing reactive power, and Figure 3(b) shows STATCOM generating reactive power.

When the voltage drops or rises to a specific value, the STATCOM is limited by the capacity required by the train. The control system will act on the semiconductor valves to maintain a stable state with no shortage or surplus of reactive power. Therefore, the output current remains unchanged, and the reactive power is controlled by continuously adjusting the amplitude and phase of the V_{ST}.
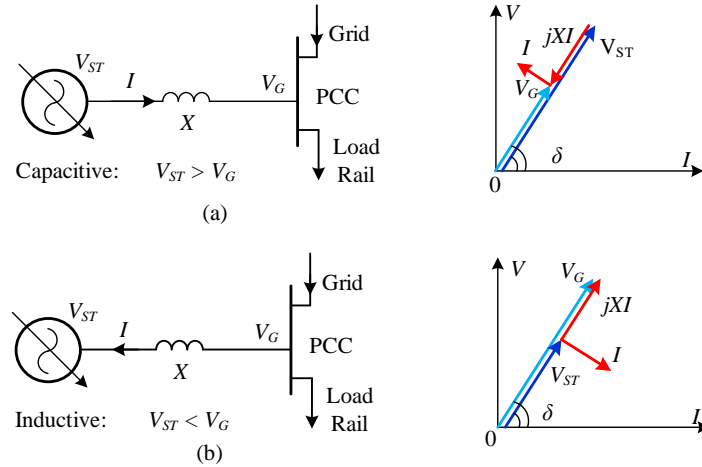
Figure 3. Diagram showing the operating principle of STATCOM: (a) absorbing reactive power and (b) emitting reactive power

3. MODELING AND CONTROL STRATEGY OF STATCOM BASED ON THREE-PHASE BRIDGE INVERTER

3.1. Mathematical model of STATCOM based on a three-phase bridge inverter

The reactive power control process for STATCOM, based on voltage value control, is performed using three-phase bridge inverter control, as shown in Figure 4. In which: i_a, i_b, i_c are the output current of STATCOM; V_{ST_a}, V_{ST_b}, V_{ST_c} are the output voltage of the converter; V_{G_a}, V_{G_b}, V_{G_c} are the voltage at PCC; V_{dc} is the DC voltage of STATCOM; i_{dc} is the DC current of STATCOM; L is the inductance of the transformer; R is the resistance of the transformer.
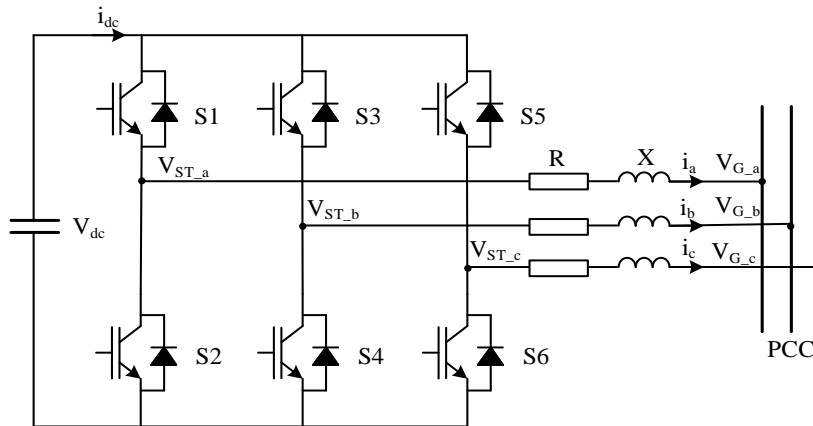

Figure 4. STATCOM structure based on a three-phase bridge inverter

From Figure 4, we can write the relationship between the DC and AC side currents of STATCOM as (8).

$$i_{dc} = \begin{bmatrix} D_a - D_b \\ D_b - D_c \\ D_c - D_a \end{bmatrix}^T \begin{bmatrix} i_{ab} \\ i_{bc} \\ i_{ca} \end{bmatrix} \tag{8}$$

Where: D_k are the functional conversion factors and $k = a, b, c$.

$$i_{ab} = \frac{1}{3}(i_a - i_b), i_{bc} = \frac{1}{3}(i_b - i_c), i_{ca} = \frac{1}{3}(i_c - i_b) \text{ and } \begin{bmatrix} V_{ST\_a} - V_{ST\_b} \\ V_{ST\_b} - V_{ST\_c} \\ V_{ST\_c} - V_{ST\_a} \end{bmatrix} = \begin{bmatrix} D_a - D_b \\ D_b - D_c \\ D_c - D_a \end{bmatrix} V_{dc} \tag{9}$$

$$\begin{cases} Ri_a + L\frac{di_a}{dt} = V_{G\_a} - V_{ST\_a} \\ Ri_b + L\frac{di_b}{dt} = V_{G\_b} - V_{ST\_b} \\ Ri_c + L\frac{di_c}{dt} = V_{G\_c} - V_{ST\_c} \\ L\frac{di_{ab}}{dt} = \frac{1}{3}L\left[\frac{di_a}{dt} - \frac{di_b}{dt}\right] \end{cases} \tag{10}$$

The circuit diagram in Figure 4 shows the relationship between the STATCOM output voltage and the grid voltage as in (10). The (9) and (10) can be expressed as (11) and (12).

$$\begin{cases} L\frac{di_{ab}}{dt} = \frac{1}{3}\left[(V_{G\_a} - V_{ST\_a}) - (V_{G\_b} - V_{ST\_b})\right] - i_{ab}R = \frac{1}{3}\left[(V_{G\_a} - V_{G\_b}) - (V_{ST\_a} - V_{ST\_b})\right] - i_{ab}R \\ L\frac{di_{bc}}{dt} = \frac{1}{3}\left[(V_{G\_b} - V_{G\_c}) - (V_{ST\_b} - V_{ST\_c})\right] - i_{bc}R \\ L\frac{di_{ca}}{dt} = \frac{1}{3}\left[(V_{G\_c} - V_{G\_a}) - (V_{ST\_c} - V_{ST\_a})\right] - i_{ca}R \end{cases} \tag{11}$$

$$\frac{d}{dt}\begin{bmatrix} i_{ab} \\ i_{bc} \\ i_{ca} \end{bmatrix} = \frac{1}{3L}\begin{bmatrix} V_{G\_a} - V_{G\_b} \\ V_{G\_b} - V_{G\_c} \\ V_{G\_c} - V_{G\_a} \end{bmatrix} - \frac{1}{3L}\begin{bmatrix} V_{ST\_a} - V_{ST\_b} \\ V_{ST\_b} - V_{ST\_c} \\ V_{ST\_c} - V_{ST\_a} \end{bmatrix} - \frac{R}{L}\begin{bmatrix} i_{ab} \\ i_{bc} \\ i_{ca} \end{bmatrix} \tag{12}$$

Applying equations from (9) to (12) will give (13) and (14).

$$\frac{d}{dt}\begin{bmatrix} i_{ab} \\ i_{bc} \\ i_{ca} \end{bmatrix} = \frac{1}{3L}\begin{bmatrix} V_{G\_a} - V_{G\_b} \\ V_{G\_b} - V_{G\_c} \\ V_{G\_c} - V_{G\_a} \end{bmatrix} - \frac{1}{3L}\begin{bmatrix} D_a - D_b \\ D_{bp} - D_c \\ D_c - D_a \end{bmatrix} V_{dc} - \frac{R}{L}\begin{bmatrix} i_{ab} \\ i_{bc} \\ i_{ca} \end{bmatrix} \tag{13}$$

$$C\frac{dV_{dc}}{dt} = i_p = \begin{bmatrix} D_a - D_b \\ D_b - D_c \\ D_c - D_a \end{bmatrix}^T \begin{bmatrix} i_{ab} \\ i_{bc} \\ i_{ca} \end{bmatrix} \tag{14}$$

$$\begin{bmatrix} i_d \\ i_q \\ 0 \end{bmatrix} = \frac{2}{3}\begin{bmatrix} \cos(\omega t) & \cos\left(\omega t - \frac{2}{3}\pi\right) & \cos\left(\omega t + \frac{2}{3}\pi\right) \\ -\sin(\omega t) & -\sin\left(\omega t - \frac{2}{3}\pi\right) & -\sin\left(\omega t + \frac{2}{3}\pi\right) \\ \frac{1}{2} & \frac{1}{2} & \frac{1}{2} \end{bmatrix} \tag{15}$$

The (14) is commonly used in power systems to convert three-phase to two-phase in a rotating reference frame. For the convenience of control with the proposed strategy, the Park transformation is used to convert the *abc* coordinate system of (14) to the *dq* coordinate system. From power system theory, we will get the effective and reactive currents relative to a rotating reference frame with angular frequency ω in the *dq* coordinate system as in (15). In this case, i_d is the active current component, and i_q is the reactive current component. Then will get (16).

$$\begin{bmatrix} i_{ab} \\ i_{bc} \\ i_{ca} \end{bmatrix} = \frac{1}{3}\begin{bmatrix} i_a - i_b \\ i_b - i_c \\ i_c - i_a \end{bmatrix} = \frac{1}{3}\left(\begin{bmatrix} i_a \\ i_b \\ i_c \end{bmatrix} - \begin{bmatrix} i_b \\ i_c \\ i_a \end{bmatrix}\right) = \frac{1}{\sqrt{3}}\begin{bmatrix} -\sin\left(\omega t - \frac{1}{3}\pi\right) & \cos\left(\omega t - \frac{1}{3}\pi\right) & 1 \\ \sin(\omega t) & -\cos(\omega t) & 1 \\ -\sin\left(\omega t + \frac{1}{3}\pi\right) & \cos\left(\omega t + \frac{1}{3}\pi\right) & 1 \end{bmatrix}^{-1}\begin{bmatrix} i_d \\ i_q \\ 0 \end{bmatrix} \tag{16}$$

Set $T^{-1} = \frac{1}{\sqrt{3}}\begin{bmatrix} -\sin\left(\omega t - \frac{1}{3}\pi\right) & \cos\left(\omega t - \frac{1}{3}\pi\right) & 1 \\ \sin(\omega t) & -\cos(\omega t) & 1 \\ -\sin\left(\omega t + \frac{1}{3}\pi\right) & \cos\left(\omega t + \frac{1}{3}\pi\right) & 1 \end{bmatrix}$

Then we have: $\begin{bmatrix} i_d \\ i_q \end{bmatrix} = T\begin{bmatrix} i_{ab} \\ i_{bc} \\ i_{ac} \end{bmatrix}$; $\begin{bmatrix} V_{G\_d} \\ V_{G\_q} \end{bmatrix} = T\begin{bmatrix} V_{G\_ab} \\ V_{G\_bc} \\ V_{G\_ac} \end{bmatrix}$; $\begin{bmatrix} D_d \\ D_q \end{bmatrix} = T\begin{bmatrix} D_{ab} \\ D_{bc} \\ D_{ac} \end{bmatrix}$ (17)

From the transformation of (17) to the left side of (16), we get (18).

$$\frac{d}{dt}\begin{bmatrix} i_{ab} \\ i_{bc} \\ i_{ac} \end{bmatrix} = \frac{d\left(T^{-1}\begin{bmatrix} i_d \\ i_q \end{bmatrix}\right)}{dt} = \frac{dT^{-1}}{dt}\begin{bmatrix} i_d \\ i_q \end{bmatrix} + T^{-1}\begin{bmatrix} \frac{di_d}{dt} \\ \frac{di_q}{dt} \end{bmatrix} \tag{18}$$

Similar to the above transformation, the (19) can be derived.

$$\frac{dT^{-1}}{dt}\begin{bmatrix} i_d \\ i_q \end{bmatrix} + T^{-1}\begin{bmatrix} \frac{di_d}{dt} \\ \frac{di_q}{dt} \end{bmatrix} = \frac{1}{3L}T^{-1}\begin{bmatrix} V_{G\_d} \\ V_{G\_q} \end{bmatrix} - \frac{1}{3L}T^{-1}\begin{bmatrix} D_d \\ D_q \end{bmatrix} \cdot V_{dc} - \frac{R}{L}T^{-1}\begin{bmatrix} i_d \\ i_q \end{bmatrix} \tag{19}$$

From the principle of electrical systems, it can be inferred as (20).

$$V_{G\_d} = V_m; V_{G\_q} = 0; \ T\frac{dT^{-1}}{dt}\begin{bmatrix} 0 & -\omega \\ \omega & 0 \end{bmatrix} \tag{20}$$

Multiply T by both sides of (19) and apply (20) to get (21).

$$\begin{bmatrix} \frac{di_d}{dt} \\ \frac{di_q}{dt} \end{bmatrix} = \begin{bmatrix} \frac{-R}{L} & \omega & \frac{-D_d}{3L} \\ \omega & \frac{-R}{L} & \frac{-D_q}{3L} \end{bmatrix}\begin{bmatrix} i_d \\ i_q \\ V_{dc} \end{bmatrix} + \begin{bmatrix} \frac{1}{3L} \\ 0 \\ 0 \end{bmatrix}V_m \tag{21}$$

Rearranging (20) and (21) will get the relationship between current and voltage in the *dq* coordinate system as (22).

$$\begin{cases} \frac{di_d}{dt} = \frac{-R}{L}i_d + i_q\omega - \frac{V_{dc}}{3L}D_d + \frac{1}{3L}V_m \\ \frac{di_q}{dt} = -i_d\omega - \frac{R}{L}i_q - \frac{V_{dc}}{3L}D_q \\ \frac{dV_{dc}}{dt} = \frac{3}{2C}i_dD_d + \frac{3}{2C}i_qD_a \end{cases} \tag{22}$$

$$\frac{d}{dt}\begin{bmatrix} i_d \\ i_q \\ V_{dc} \end{bmatrix} = \begin{bmatrix} \frac{-R}{L} & \omega & \frac{-D_d}{3L} \\ -\omega & \frac{-R}{L} & \frac{-D_q}{3L} \\ \frac{2}{3C}D_d & \frac{2}{3C}D_q & 0 \end{bmatrix}\begin{bmatrix} i_d \\ i_q \\ V_{dc} \end{bmatrix} + \begin{bmatrix} \frac{1}{3L} \\ 0 \\ 0 \end{bmatrix}V_m \tag{23}$$

The (22) shows that the coefficient D_k is flexible and can be used in the model as a control variable to control the parameters i_d, i_q, and V_{dc}.

3.2. Control model for STATCOM reactive power compensation for high-speed trains

The STATCOM in Figure 5 is an independent power source fed into the connection point to control the voltage imbalance and reactive power in order to improve the train's power quality. This paper proposes a control system using two loops to realize reactive power control for the train. The parameters of the AC power system are converted through the dq coordinate system into DC components to simplify the control process. In the case of ignoring the effects of disturbances.

Figure 5 shows that the 3-phase AC voltage and current will be measured and converted to dq coordinates through the phase-locked loop in the PLL block, and the DC voltage of the STATCOM is also measured. After the voltage value is converted from the abc coordinate system to the *dq* coordinate system through the abc/dc block, these quantities will be compared with their reference values, and static errors will be eliminated through the linear PI controller. The loop system uses two controllers and is explicitly described as follows:

−   DC voltage regulator: The DC voltage value V_{dc} is measured from STATCOM, then compared with the reference DC voltage value V_{dc_ref}, the error between the actual value and the reference value of the DC voltage is fed into the PI controller to cancel and create a reference current value i_{d_ref}, this current is used to compare with the current i_{ST_d}, the comparison process will determine the error value and be canceled by the PI controller and create a reference value i_{d_ref}, the i_{d_ref} current is the component in phase with the voltage used to control the active power flow.

−   AC voltage regulator: After determining V_{G_d} and V_{G_q} in the *dq* coordinate system, the process calculates their amplitudes and compares them with the reference value V_{ref}. The comparison process determines the deviation value, which the PI controller eliminates. The PI controller creates the reference current i_{q_ref} to

control the reactive current. The i_{q_ref} current is the component perpendicular to the voltage, regulating the reactive power flow.

After having the set values of the reference current i_{d_ref} and i_{q_ref}, they will be compared with the values of the actual current i_{ST-d} and i_{ST-q}; the error values of this comparison process will be eliminated by the PI controller of the inner loop and create control voltages v_d and v_q. By converting from dq coordinates to abc coordinates in block dq/abc will get the control voltages v_a, v_b, v_c. These signals will be fed into the PWM stage to create the IGBT valve switching pulse of the STATCOM to create the desired reactive power and maintain the stability of the system voltage to supply the train system, while being able to synchronize the appropriate operating power to stabilize the voltage on the DC side.
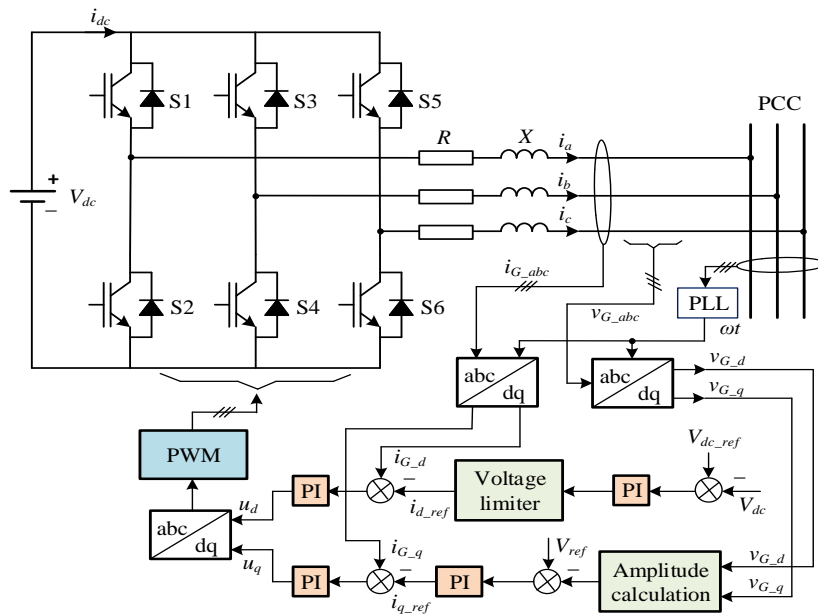

Figure 5. STATCOM control system diagram

4. SIMULATION AND EVALUATION OF RESULTS

The system is simulated with the parameters shown in Tables 1 and 2. Table 1 shows the parameters of the train, and Table 2 shows the parameters of the STATCOM device. Figure 6 illustrates the reference and feedback speed curves. The speed curve deviates from the reference one during the transition from the acceleration phase to the constant speed phase. However, the feedback curve subsequently follows the reference closely.

Table 1. Parameters of high-speed train

Parameters of the train	Speed (rpm)	Power (kW)	Parameters of the train	Speed (rpm)	Power (kW)
Mass of train at full load (M)	494000	kg	Coefficient C	0.00095561	
Number of motors (N)	8		Wheel diameter (Dwh)	0.84	m
Maximum speed (Vmax)	350	km/h	Transmission ratio (i)	107/16	
Base speed (Vb)	320	km/h	Gearbox performance	0.85	
Coefficient A	1.6		Motor performance	0.95	
Coefficient B	0.035		Inertia moment of train (J)	343.561	kg.m2

Table 2. Parameters of STACOM

Parameters of STACOM	Value
Transformer rated voltage	2.5/30 kV
Rated frequency	50 Hz
PWM frequency	5000 Hz
Apparent rated power	3–15 MVA
Resistance	0.22/30 pu
Inductance	0.22 pu
Voltage V_{ST} STATCOM	2000 V
Continuous DC tension	4000 V

The train's current and voltage are always stable in operating modes, as shown in Figures 7 and 8 have a standard sinusoidal form when the train's speed changes in Figure 6. This proves that when the system is compensated, the current and voltage at the PCC point supplying power to the load are always stable and balanced, even though the grid voltage fluctuates. The quality of current and voltage, as in Figures 9(a) and 9(b), shows that the THD of the current is 1.95%, and the THD of the voltage is 0.1%. Referring to the IEEE 519 standard, these are values that represent suitable power quality. These indices ensure that the quality of power supplied to the train is consistently guaranteed, allowing the traction motors to operate efficiently for an extended period.
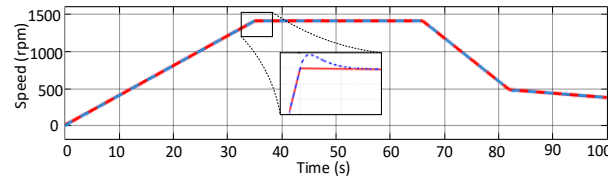
Figure 6. Speed curve of the train
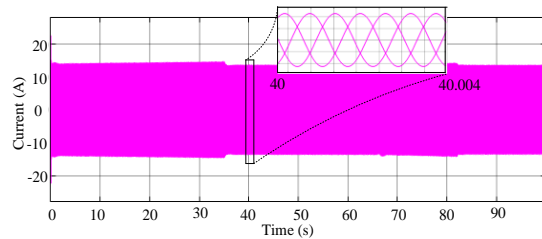
Figure 7. Current at PCC supplied to the load after reactive power compensation
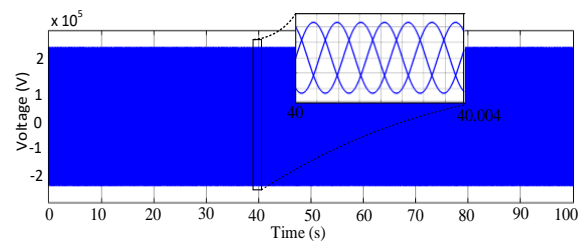
Figure 8. Voltage at PCC supplied to the load after reactive power compensation
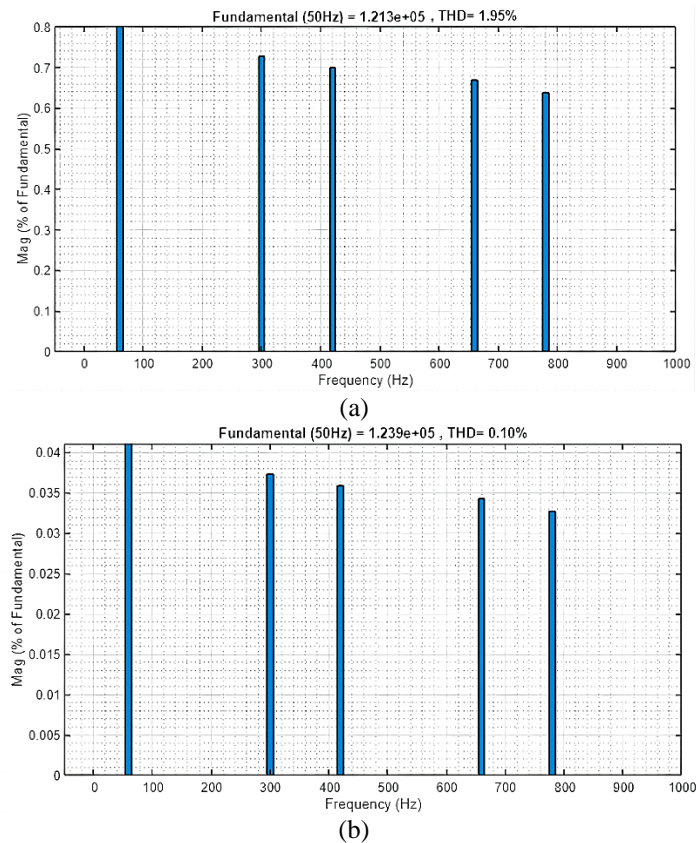

(a)

(b)

Figure 9. THD values of (a) current and (b) voltage at the PPC point

Figure 10 is the result of the DC voltage value of STATCOM. This result indicates that the DC voltage remains stable in the high-speed train's operating modes. When the high-speed train changes its operating mode, as shown in Figure 6, the DC voltage fluctuates insignificantly. This demonstrates that the controller has maintained a consistently stable DC voltage without any significant transients.

Figure 11 is the result of reactive power compensation at the PPC point when the operating mode of the grid and the train change. The result shows that when the grid and the train change operating modes, the STATCOM compensates for a certain amount of power, as illustrated in Figure 11(a), to provide sufficient reactive power for the train load to remain stable, as shown in Figure 11(b). This result demonstrates that the PI controller has responded promptly to supply reactive power to the train, ensuring stable operation. Figure 12 illustrates the active power exchanged between the STATCOM and the grid at the PPC point. The results show that during the operation of the high-speed train, the active power exchanged by the STATCOM with the grid is always close to zero, which confirms that the control design process for the STATCOM has met demands for the set goal.
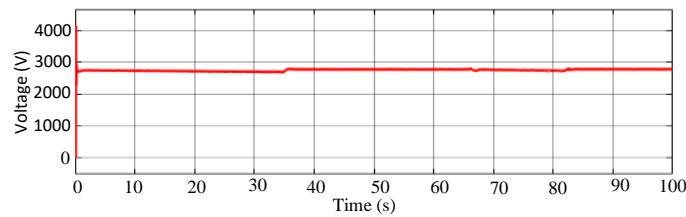

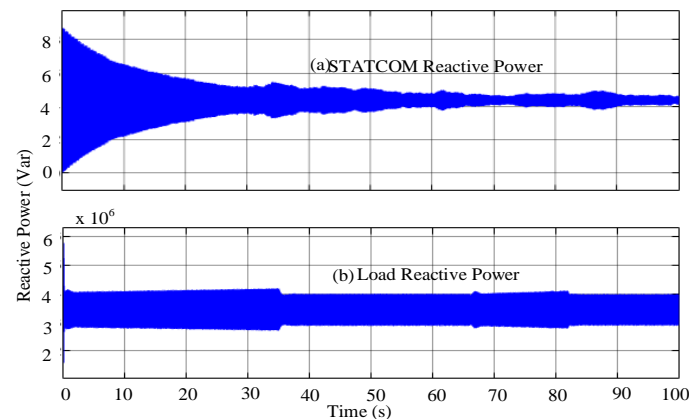Figure 10. DC side voltage of STATCOM

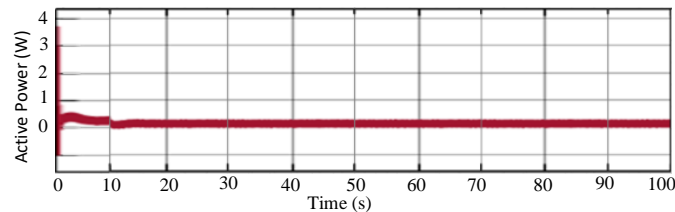Figure 11. Reactive power: (a) output of STATCOM and (b) on load

Figure 12. Active output power of STATCOM

5. CONCLUSION

The paper presents the model and method of reactive power control applied to high-speed train systems. The paper analyses the importance of high-speed passenger trains. It then examines the mathematical model of the power electronic converter applied to the STATCOM device, including its operating principles for compensating reactive power. Finally, the design of the reactive power control

system based on the three-phase bridge converter model instantly provides the missing reactive power of the high-speed train. Providing sufficient reactive power will ensure a stable operating voltage; on the other hand, making the voltage supplied to the train stable and continuous for a long time will reduce energy losses and increase the life of the electric motor and help the passenger transport process better. The simulation results of the control process when the system is operating have shown that when the voltage at the supply node for the train fluctuates due to the phenomenon of reactive power shortage, the STATCOM device can control the compensation of the appropriate amount of power to stabilize the voltage at the PCC node. The results have shown that the reactive power value effectively follows the desired setting value, limiting the voltage drop process, improving the stability and reliability of power supply for high-speed trains. This has confirmed the correctness of the theoretical analysis presented in the paper.

FUNDING INFORMATION

AUTHOR CONTRIBUTIONS STATEMENT
This journal uses the Contributor Roles Taxonomy (CRediT) to recognize individual author contributions, reduce authorship disputes, and facilitate collaboration.

Name of Author	C	M	So	Va	Fo	I	R	D	O	E	Vi	Su	P	Fu
An Thi Hoai Thu Anh	✓	✓	✓	✓	✓	✓		✓	✓	✓		✓	✓	✓
Tran Hung Cuong		✓	✓	✓		✓	✓		✓		✓		✓	

C : **C**onceptualization	I : **I**nvestigation	Vi : **Vi**sualization
M : **M**ethodology	R : **R**esources	Su : **Su**pervision
So : **So**ftware	D : **D**ata Curation	P : **P**roject administration
Va : **Va**lidation	O : Writing - **O**riginal Draft	Fu : **Fu**nding acquisition
Fo : **Fo**rmal analysis	E : Writing - Review & **E**diting	

CONFLICT OF INTEREST STATEMENT
Authors state no conflict of interest.

DATA AVAILABILITY
All data supporting the findings of this study are included in this published article.

REFERENCES
[1]   B. Gavrilovic and V. A. Baboshin, "Simulations of the operation of the fast light innovative regional train from 'Serbian Railways' in traction and electric braking mode," *Mechanical Engineering Advances*, vol. 2, no. 1, p. 1214, Nov. 2023, doi: 10.59400/mea.v2i1.1214.
[2]   R. Brkić, Ž. Adamović, and M. Bukvić, "Modeling of reliability and availability of data transmission in railway system," *Advanced Engineering Letters*, vol. 1, no. 4, pp. 136–141, 2022, doi: 10.46793/adeletters.2022.1.4.3.
[3]   L. Barros, M. Tanta, A. Martins, J. Afonso, and J. Pinto, "Evaluation of static synchronous compensator and rail power conditioner in electrified railway systems using V/V and Scott power transformers," *EAI Endorsed Transactions on Energy Web*, Jul. 2021, doi: 10.4108/eai.29-3-2021.169164.
[4]   S. M. Tripathi and P. J. Barnawal, "Design and control of a STATCOM for non-linear load compensation: a simple approach," *Electrical, Control and Communication Engineering*, vol. 14, no. 2, pp. 172–184, 2018, doi: 10.2478/ecce-2018-0021.
[5]   M. Zhang, Q. Zhang, Y. Lv, W. Sun, and H. Wang, "An AI based high-speed railway automatic train operation system analysis and design," in *2018 International Conference on Intelligent Rail Transportation (ICIRT)*, Dec. 2018, pp. 1–5. doi: 10.1109/ICIRT.2018.8641650.
[6]   J. Guzinski, M. Diguet, Z. Krzeminski, A. Lewicki, and H. Abu-Rub, "Application of speed and load torque observers in high-speed train drive for diagnostic purposes," *IEEE Transactions on Industrial Electronics*, vol. 56, no. 1, pp. 248–256, Jan. 2009, doi: 10.1109/TIE.2008.928103.
[7]   J. Xue *et al.*, "Speed tracking control of high-speed train based on particle swarm optimization and adaptive linear active disturbance rejection control," *Applied Sciences*, vol. 12, no. 20, p. 10558, Oct. 2022, doi: 10.3390/app122010558.
[8]   H. Chen and B. Jiang, "A review of fault detection and diagnosis for the traction system in high-speed trains," *IEEE Transactions on Intelligent Transportation Systems*, vol. 21, no. 2, pp. 450–465, Feb. 2020, doi: 10.1109/TITS.2019.2897583.
[9]   Q. Yan, I. A. Tasiu, H. Chen, Y. Zhang, S. Wu, and Z. Liu, "Design and hardware-in-the-loop implementation of fuzzy-based proportional-integral control for the traction line-side converter of a high-speed train," *Energies*, vol. 12, no. 21, p. 4094, Oct. 2019, doi: 10.3390/en12214094.

[10] A. M. Eltamaly, A. Nasr, A. Elghaffar, A.-H. Ahmed, Y. Sayed, and A.-H. M. El-Sayed, "Enhancement of power system quality using static synchronous compensation (STATCOM)," *International Journal of Mechatronics, Electrical and Computer Technology (IJMEC)*, vol. 8, no. 30, pp. 3966–3974, 2018, [Online]. Available: www.aeuso.org

[11] A. M. Ibrahim, S. A. Gawish, N. H. El-Amary, and S. M. Sharaf, "STATCOM controller design and experimental investigation for wind generation system," *IEEE Access*, vol. 7, pp. 150453–150461, 2019, doi: 10.1109/ACCESS.2019.2946141.

[12] F. Luan, Y. Zhang, L. Xiao, C. Zhou, and S. Zhou, "Fading characteristics of wireless channel on high-speed railway in hilly terrain scenario," *International Journal of Antennas and Propagation*, vol. 2013, no. 1, 2013, doi: 10.1155/2013/378407.

[13] L. A. M. Barros, M. Tanta, A. P. Martins, J. L. Afonso, and J. G. Pinto, "STATCOM evaluation in electrified railway using V/V and Scott power transformers," in *International Conference on Sustainable Energy for Smart Cities*, 2019, pp. 18–32. doi: 10.1007/978-3-030-45694-8_2.

[14] A. Benslimane, J. Bouchnaif, M. Azizi, and K. Grari, "Study of a STATCOM used for unbalanced current compensation caused by a high speed railway (HSR) sub-station," in *2013 International Renewable and Sustainable Energy Conference (IRSEC)*, Mar. 2013, pp. 441–446. doi: 10.1109/IRSEC.2013.6529724.

[15] J. A. Suul, M. Molinas, and T. Undeland, "STATCOM-based indirect torque control of induction machines during voltage recovery after grid faults," *IEEE Transactions on Power Electronics*, vol. 25, no. 5, pp. 1240–1250, May 2009, doi: 10.1109/TPEL.2009.2036619.

[16] A. Sharma and H. Singh, "MATLAB simulation of D-STATCOM using SVPWM," *International Journal of Engineering Technologies and Management Research*, vol. 5, no. 5, pp. 184–195, Feb. 2020, doi: 10.29121/ijetmr.v5.i5.2018.240.

[17] N. Izadpanahi, B. Fani, A. Etesami, M. Mahdavian, and S. Javadi, "DFIG-based wind turbine using STATCOM for improvement performance," in *2017 14th International Conference on Electrical Engineering/Electronics, Computer, Telecommunications and Information Technology (ECTI-CON)*, Jun. 2017, pp. 396–399. doi: 10.1109/ECTICon.2017.8096257.

[18] Q. Wu, Q. Jiang, and Y. Wei, "Study on railway unified power quality controller based on STATCOM technology," in *2011 5th International Power Engineering and Optimization Conference*, Jun. 2011, pp. 297–300. doi: 10.1109/PEOCO.2011.5970452.

[19] V. D. Ram and M. Chidambaram, "Simple method of designing centralized PI controllers for multivariable systems based on SSGM," *ISA Transactions*, vol. 56, pp. 252–260, May 2015, doi: 10.1016/j.isatra.2014.11.019.

[20] F. F. Panoeiro, M. F. Santos, D. C. Silva, J. L. Silva, and M. J. Carmo, "PI controller tuned by bee swarm for level control systems," in *2018 19th International Carpathian Control Conference (ICCC)*, May 2018, pp. 301–306. doi: 10.1109/CarpathianCC.2018.8399645.

[21] L. R. da Silva, R. C. C. Flesch, and J. E. Normey-Rico, "Analysis of anti-windup techniques in PID control of processes with measurement noise," *IFAC-PapersOnLine*, vol. 51, no. 4, pp. 948–953, 2018, doi: 10.1016/j.ifacol.2018.06.100.

[22] A. S. Samosir, T. Sutikno, and L. Mardiyah, "Simple formula for designing the PID controller of a DC-DC buck converter," *International Journal of Power Electronics and Drive Systems (IJPEDS)*, vol. 14, no. 1, pp. 327–336, Mar. 2023, doi: 10.11591/ijpeds.v14.i1.pp327-336.

[23] Z. Yi, Z. Yang, S. Li, F. Lin, and W. Liu, "Study on the control method of high-speed train traction motor continuous load," in *1st International Workshop on High-Speed and Intercity Railways*, 2012. doi: 10.1007/978-3-642-27960-7_42.

[24] P. Rodrigues, V. A. Morais, A. Martins, and A. Carvalho, "STATCOM simulation models for analysis of electrified railways," in *IECON 2019 - 45th Annual Conference of the IEEE Industrial Electronics Society*, Oct. 2019, pp. 2257–2262. doi: 10.1109/IECON.2019.8927256.

[25] A. M. Obais and A. A. Mukheef, "Design of a linearized 4-H-bridge STATCOM for load balancing purposes," *International Journal of Power Electronics and Drive Systems (IJPEDS)*, vol. 14, no. 4, pp. 2080–2093, Dec. 2023, doi: 10.11591/ijpeds.v14.i4.pp2080-2093.

BIOGRAPHIES OF AUTHORS

An Thi Hoai Thu Anh 🆔 🔗 SC 🔗 received her Engineer (1997), M.Sc. (2002) degrees in industrial automation engineering from Hanoi University of Science and Technology, and completed her Ph.D. degree in 2020 from the University of Transport and Communications (UTC). Now, she is a lecturer of the Faculty of Electrical and Electronic Engineering under the University of Transport and Communications (UTC). Her current interests include power electronic converters, electric motor drives, saving energy-saving solutions applied to industry and transportation. She can be contacted at email: htanh.ktd@utc.edu.vn.

Tran Hung Cuong 🆔 🔗 SC 🔗 received his Engineer (2010), M.Sc. (2013) degrees in industrial automation engineering from Hanoi University of Science and Technology, and completed his Ph.D. degree in 2020 from Hanoi University of Science (HUST). Now, he is a lecturer of the Faculty of Electrical and Electronic Engineering under Thuyloi University (TLU). His current interests include power electronic converters, electric motor drives, converting electricity from renewable energy sources to the grid, and saving energy solutions applied to the grid and transportation. He can be contacted at email: cuongth@tlu.edu.vn.